CROATICA CHEMICA ACTA CCACAA **68** (4) 745–767 (1995)

ISSN 0011-1643
CCA–2269
Original Scientific Paper

Synthesis and Characterisation of $[Pd_{10}(\mu\text{-}CO)_8(\mu_3\text{-}CO)_4(PEt_3)_6]$ and $[Pd_{10}(\mu\text{-}CO)_6(\mu_3\text{-}CO)_2(\mu\text{-}CNXylyl)_2(PEt_3)_6]$

D. Michael P. Mingos and Christopher M. Hill*

Chemistry Department, Imperial College of Science, Technology and Medicine,
South Kensington, London SW7 2AY, United Kingdom

Received January 16, 1995; accepted January 27, 1995

The decanuclear palladium cluster compounds $[Pd_{10}(\mu\text{-}CO)_8(\mu_3\text{-}CO)_4(PEt_3)_6]$ and $[Pd_{10}(\mu\text{-}CO)_6(\mu_3\text{-}CO)_2(\mu\text{-}CNXyl)_2(PEt_3)_6]$ (Xyl = $C_6H_3Me_2$-2,6) have been synthesised and characterised by a combination of spectroscopic data and single crystal X-ray crystallographic analyses. The former has a distorted tetracapped octahedral skeletal geometry and the latter a hexacapped tetrahedral geometry. The latter is unique in cluster chemistry and the structural change induced by the addition of isocyanide represents an interesting example of the effect of the steric requirements of the isocyanide ligand influencing the total electron count and geometry of the cluster. $[Pd_{10}(\mu\text{-}CO)_8(\mu_3\text{-}CO)_4(PEt_3)_6]$ reacts with SO_2 to give $[Pd_5(\mu\text{-}SO_2)_2(\mu_3\text{-}SO_2)_2(PEt_3)_5]$.

INTRODUCTION

The compound $[Pd_2(dba)_3]$.Sol (Sol = $CHCl_3$, dba = dibenzylideneacetone) has proved to be of great use in the synthesis of medium to large palladium cluster compounds.[1] $[Pd_2(dba)_3]$.Sol undergoes aggregation reactions in the presence of a wide variety of ligands, including phopshines, isocyanides and sulphur dioxide, to form clusters such as $[Pd_8(\mu\text{-}CO)_6(\mu_3\text{-}CO)_2(PMe_3)_7]$,[2] $[Pd_5(\mu\text{-}SO_2)_2(\mu_3\text{-}SO_2)_2(PPh_3)_5]$,[3] and $[Pd_5(\mu\text{-}SO_2)_3(\mu\text{-}CNXyl)_2(CNXyl)_5]$.[4] The palladium(II) compound $[Pd_3(\mu\text{-}OAc)_6]$ has been used by Mednikov and co-workers[5–10] to synthesise a range of cluster compounds, including

---

* Author to whom correspondence should be addressed.

$[Pd_4(\mu\text{-}CO)_5(PBu_3)_4]$, $[Pd_4(\mu\text{-}CO)_6(PBu_3)_4]$ and $[Pd_{10}(\mu\text{-}CO)_8(\mu_3\text{-}CO)_4(PBu_3)_6]$. It has also been used in the synthesis of the large palladium cluster compounds, $[Pd_{23}(\mu\text{-}CO)_{14}(\mu_3\text{-}CO)_8(PEt_3)_{10}]$ and $[Pd_{38}(\mu\text{-}CO)_{24}(\mu_3\text{-}CO)_4(PEt_3)_{12}]$, by reaction with the medium sized cluster $[Pd_{10}(\mu\text{-}CO)_8(\mu_3\text{-}CO)_4(PEt_3)_6]$.

$[Pd_8(\mu\text{-}CO)_6(\mu_3\text{-}CO)_2(PMe_3)_7]$,[2] $[Pd_{10}(\mu\text{-}CO)_8(\mu_3\text{-}CO)_4(CO)_2(PBu_3)_4]$[10] and $[Pd_{10}(\mu\text{-}CO)_8(\mu_3\text{-}CO)_4(PBu_3)_6]$[5] have geometries based on octahedra with face capping palladium atoms, $[Pd_{23}(\mu\text{-}CO)_{14}(\mu_3\text{-}CO)_8)PEt_3)_{10}]$[6] and $[Pd_{23}(\mu\text{-}CO)_{16}(\mu_3\text{-}CO)_4(PEt_3)_8]$[7] have geometries based on cubic close packed and body centred packing arrangements. $[Pd_{38}(\mu\text{-}CO)_{24}(\mu_3\text{-}CO)_4(PEt_3)_{12}]$[8] has a structure which cannot be simply described in terms of close packed arrangements and is best described in terms of a central tetrahedron surrounded by 20 palladium atoms in four approximately planar layers and two interstitial palladium atoms. $[Pd_{16}(\mu\text{-}CO)_6(\mu_3\text{-}CO)_7(PEt_3)_9]$[9] has a structure based on an icosahedron of Pd_{13} with three bridging $Pd(CO)(PEt_3)$ fragments.

Although we have previously studied in some detail the reactions of low nuclearity palladium clusters with isocyanide ligands the corresponding reactions of high nuclearity cluster compounds have been neglected.[1]

EXPERIMENTAL

General Procedures

The reactions were routinely carried out using standard Schlenk line techniques under an atmosphere of pure dry dinitrogen with dry and dioxygen free solvents. Microanalyses (C, H, N, Pd) were carried out by Mr. M. Gascoyne and his staff at Inorganic Chemistry Laboratory, Oxford University. Infrared spectra were recorded on a Perkin Elmer FT – 1710 Spectrometer as nujol mulls and recorded between KBr discs. $^{31}P\{^1H\}$-NMR spectra were recorded on an Bruker AM-300 spectrometer operating at a frequency of 121.49 MHz and referenced to $PO(OMe)_3$ in D_2O. $^{31}P[^1H]$-NMR solid state spectra (CP/MAS) were measured by Dr. S. Mason at Oxford University on a Bruker MSL-200 spectrometer operating at 80.96 MHz. The FAB Mass Spectra were recorded by Dr. J. Ballantine and his staff at the SERC Mass Spectrometry Service Centre at the University of Swansea.

Crystallography

Intensity data were measured with an Enraf-Nonius CAD4 diffractometer at the Chemical Crystallography Laboratory, Oxford University. The collection was carried out at 293 K using molybdenum radiation (Mo Kα, $\lambda = 0.71069$Å). The goniometer software was run directly from a DEC MicroVAX 3300. The same computer was used for the subsequent steps involved in the structure analysis. A structure solution was obtained using SHELXS86.[11] Refinement was carried out using CRYSTALS suite of programs.[12] The atomic scattering factors were taken from Ref. 13.

Synthesis of $[Pd_{10}(\mu\text{-}CO)_8(\mu_3\text{-}CO)_4(PEt_3)_6]$

$[Pd_2(dba)_3]\cdot CHCl_3$ (1.75 g, 1.69 mmol) was dissolved in CH_2Cl_2 (40 cm^3) and PEt_3 (3 cm^3 of a 1 M solution, in THF) was introduced into the mixture using a syringe, under dinitrogen. CO was bubbled through the mixture for two minutes and the mixture was then stirred for 1 h under an atmosphere of CO, during which time the colour changed from purple to deep red. The solvent was then removed under reduced pressure and the crude product washed with four portions of Et_2O (30 cm^3 each). Deep purple crystals of $[Pd_{10}(\mu\text{-}CO)_8(\mu_3\text{-}CO)_4(PEt_3)_6]$ were obtained upon recrystallisation from CH_2Cl_2/Et_2O. Yield 0.52 g (73%).

IR (nujol) ν_{max}: 1891(s), 1874(m), 1853(s), 1822(w), 1793(w) (CO) cm^{-1}; $^{31}P\{^1H\}$-NMR ($CDCl_3$) δ: 9.5 ppm (4P, s), 1.18 ppm (2P, s).

Anal. Calcd. for $C_{48}H_{90}O_{12}P_6Pd_{10}$: C 27.3, H 4.3, Pd 50.5%; found: C 26.7, H 4.3, Pd 49.9%.

Synthesis of $[Pd_{10}(\mu\text{-}CO)_6(\mu_3\text{-}CO)_2(\mu\text{-}CNXyl)_2(PEt_3)_6]$

$[Pd_{10}(\mu\text{-}CO)_8(\mu_3\text{-}CO)_4(PEt_3)_6]$ (0.20 g, 0.095 mmol) was dissolved in CH_2Cl_2 (30 cm^3). Xylyl isocyanide (0.025 g, 0.190 mmol) was dissolved in a separate portion of CH_2Cl_2 (20 cm^3) and was added to the first solution with stirring. The solution changed in colour immediately from a deep red/purple to dark red and this was accompanied by a light effervescence which lasted for only a few seconds. The solution was allowed to continue stirring for five minutes and the solvent was removed under reduced pressure. The crude product was soluble in all commonly available laboratory solvents, but recrystallisation was achieved from a highly concentrated hexane solution, with cooling, giving red, air-sensitive, single crystals of $[Pd_{10}(\mu\text{-}CO)_6(\mu_3\text{-}CO)_2(\mu\text{-}CNXyl)_2(PEt_3)_6]$ in small yield. Yield 0.05 g (23%).

IR (nujol) ν_{max}: 2086(m) (CN); 1951(m), 1845(m), 1723(m) (CO) cm^{-1}.

Synthesis of $[Pd_5(\mu\text{-}SO_2)_2(\mu_3\text{-}SO_2)_2(PEt_3)_5]$

Reaction of $[Pd_{10}(\mu\text{-}CO)_8(\mu_3\text{-}CO)_4(PEt_3)_6]$ with SO_2. – $[Pd_{10}(\mu\text{-}CO)_8(\mu_3\text{-}CO)_4(PEt_3)_6]$ (0.200 g, 0.095 mmol) was dissolved in CH_2Cl_2 (30 cm^3). SO_2 was bubbled through the solution for 5 minutes and stirring was continued for a further hour under an atmosphere of SO_2. The solution changed colour gradually, from deep red/purple to deep red. The solvent was removed under reduced pressure and the product extracted from the mixture with three portions of Et_2O (30 cm^3 each). The solution was concentrated by removing Et_2O under reduced pressure, yielding deep red microcrystals of the product, $[Pd_5(\mu\text{-}SO_2)_2(\mu_3\text{-}SO_2)_2(PEt_3)_5]$. Yield 0.06 g (23%).

Reaction of $[Pd_2(dba)_3] \cdot CHCl_3$ with PEt_3 and SO_2. – $[Pd_2(dba)_3]\cdot CHCl_3$ (1.000 g, 0.97 mmol) was dissolved in CH_2Cl_2 (50 cm^3). PEt_3 (2 cm^3 1 M solution in THF) was transferred to a Schlenk tube by means of a syringe, under dry dinitrogen. The solution was diluted with of CH_2Cl_2 (20 cm^3) and the resulting mixture saturated with SO_2. This solution was added to the first, with stirring, and SO_2 was bubbled through for 5 minutes. The mixture was then stirred under an SO_2 atmosphere for a further hour. The colour of the solution changed gradually from purple to deep red. The solvent was then removed under reduced pressure and the crude product washed with ten portions of hexane (30 cm^3 each) to remove the dba. Recrystallisation from a concentrated solution in Et_2O gave a deep red microcrystalline product, which could not be separated from a dba impurity, $[Pd_5(\mu\text{-}SO_2)_2(\mu_3\text{-}SO_2)_2(PEt_3)_5]\cdot 0.61dba$. Yield 0.16 g (30%).

IR (nujol) ν_{max}: 1185(m), 1164(m), 1061(s), 1050(m) (SO_2) cm^{-1}; $^{31}P\{^1H\}$-NMR ($CDCl_3$) δ: 19.3 ppm (2P, s), 9.2 ppm (2P, d), 6.1 ppm (1P, t).

Anal. Calcd. for $C_{30}H_{75}O_8P_5Pd_5S_4\cdot 0.61(C_{17}H_{14}O)$: C 31.9, H 5.5, Pd 35.0%; found C 32.0, H 5.5, Pd 33.0%.

RESULTS AND DISCUSSION

Synthesis and Characterisation of $[Pd_{10}(\mu\text{-}CO)_8(\mu_3\text{-}CO)_4(PEt_3)_6]$

When a THF solution of PEt_3 was added to a solution of $[Pd_2(dba)_3]$.Sol and CO was bubbled through the mixture, the solution changed colour from purple to deep red. After one hour, the solvent was removed under reduced pressure and the crude product washed with several portions of Et_2O. Deep purple crystals of $[Pd_{10}(\mu\text{-}CO)_8(\mu_3\text{-}CO)_4(PEt_3)_6]$ were obtained upon recrystallisation from CH_2Cl_2/Et_2O.

The formula $[Pd_{10}(CO)_{12}(PEt_3)_6]$ was constistent with the FAB-MS analysis and the low-mass *(m/z)* end of the spectrum is shown in Figure 1. The major peak assignments are given in Table I. The molecular ion peak was absent, due to the ease with which the CO ligands are lost. The highest mass peak in the spectrum corresponds to the loss of a palladium atom and two CO ligands, but it is of low intensity. The most intense peak lies towards the low-mass end of the spectrum and corresponds to the $Pd_3(CO)_3$ unit. As would be

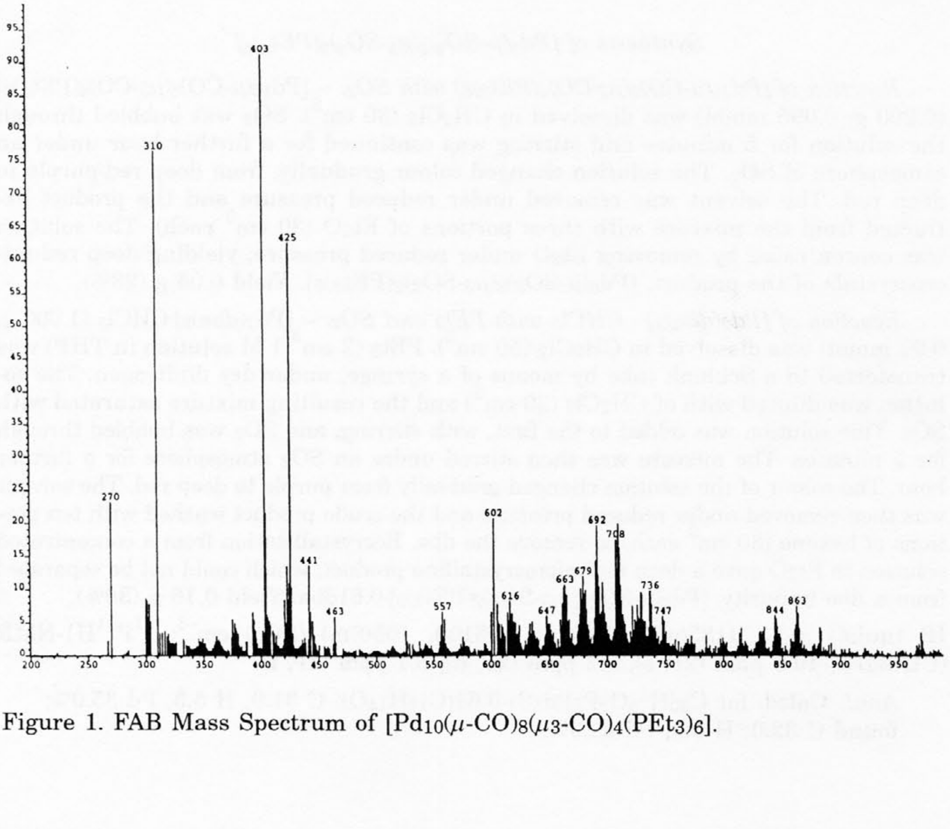

Figure 1. FAB Mass Spectrum of $[Pd_{10}(\mu\text{-}CO)_8(\mu_3\text{-}CO)_4(PEt_3)_6]$.

TABLE I

Important peaks in the assignment of the FAB-MS of $[Pd_{10}(\mu\text{-}CO)_8(\mu_3\text{-}CO)_4(PEt_3)_6]$

m/z	Intensity (rel)	Assignment
1947	<1	$[M\text{-}Pd\text{-}2CO]^+$
1745	<1	$[M\text{-}Pd\text{-}PEt_3\text{-}5CO]^+$
1395	<1	$[M\text{-}4Pd\text{-}PEt_3\text{-}6CO]^+$
1245	<1	$[M\text{-}4Pd\text{-}3PEt_3\text{-}3CO]^+$
1227	<1	$[M\text{-}4Pd\text{-}2PEt_3\text{-}8CO]^+$
1107	<1	$[M\text{-}4Pd\text{-}3PEt_3\text{-}8CO]^+$
1016	<1	$[M\text{-}4PD\text{-}4PEt_3\text{-}7CO]^+$
863	9	$[M\text{-}6Pd\text{-}3PEt_3\text{-}9CO]^+$
844	7	$[M\text{-}4Pd\text{-}5PEt_3\text{-}9CO]^+$
747	7	$[M\text{-}6Pd\text{-}4PEt_3\text{-}9CO]^+$
736	10	$[M\text{-}5Pd\text{-}5PEt_3\text{-}9CO]^+$
708	20	$[M\text{-}5Pd\text{-}5PEt_3\text{-}10CO]^+$
692	20	$[M\text{-}6Pd\text{-}4PEt_3\text{-}11CO]^+$
679	13	$[M\text{-}5Pd\text{-}5PEt_3\text{-}11CO]^+$
663	12	$[M\text{-}6Pd\text{-}4PEt_3\text{-}12CO]^+$
647	7	$[M\text{-}5Pd\text{-}5PEt_3\text{-}12CO]^+$
425	60	$[Pd(PEt_3)_2(CO)_3]^+$
403	100	$[Pd_3(CO)_3]^+$
310	75	$[Pd(PEt_3)(CO)_3]^+$
270	25	$[Pd_2(CO)_2]^+$

expected, the loss of CO is relatively facile, and all of the peaks are associated with fragments that have a large degree of CO dissociation. The presence of fragments resulting from the removal of four Pd atoms is a major feature of the central region of the spectrum, and from the crystal structure below it seems probable that these correspond to the four capping palladiums.

The low-mass end of the spectrum is dominated by small $Pd_n(CO)_m$ units.

The infra-red spectrum of the compound revealed five different ν(C-O) stretching frequencies at 1891(s), 1874(m), 1853(s), 1822(w) and 1793(w) cm^{-1}. This is consistent with the presence of both μ_2- and μ_3-bridging carbonyl ligands. Other peaks confirmed the presence of the PEt_3 ligand.

The $^{31}P\{^1H\}$-NMR spectrum revealed two singlets at 9.5 and 1.2 ppm with an approximate intensity ratio of 2 : 1 respectively. This is consistent with two distinct phosphine environments, the first being twice as abundant as the second. The crystal structure of the compound confirms this assignment, the cluster possessing four phosphines on each of the four equivalent capping palladium atoms and two on the two apical palladium atoms of the

TABLE II

Crystallographic data for the compound $[Pd_{10}(\mu\text{-}CO)_8(\mu_3\text{-}CO)_4(PEt_3)_6]$

General details	
Formula	$C_{48}H_{90}O_{12}P_6Pd_{10}$
Molecular weight	2109.08
D_c/g cm^{-3}	1.96
F(000)	4096
Linear abs. coefficient/cm^{-1}	26.0
Crystal colour	Deep red
Cell details	
Crystal system	Monoclinic
Space group	$P2_1/n$
a/Å	13.961(3)
b/Å	23.093(8)
c/Å	22.316(3)
α/°	90
β/°	96.64(2)
g/°	90
V/Å^3	7146.6
Z	4
Data collection	
X-radiation	Mo Kα, λ=0.71069 Å
$\theta_{\text{min},}$ θ_{max}/°	0.23
Min., max. h,k,l	–1, 15; –1, 25; –24, 24
ω-scan width/°	1.00 + 0.35 tanθ
Horizontal aperture/mm	3.5
Total data collected	11093
Total unique data	9956
Total observed data	4609
Merging R factor	0.060
Refinement	
Absorption correction	DIFABS (min/max = 0.67/1.48)
Number of parameters	457
Ratio data: parameters	10.2
Weighting scheme	Tukey and Prince (7.5, 0.7, 5,8, 0.1)
Final R factor	0.066
Final R_w	0.078

central octahedral unit. The lack of spin-spin coupling between the two phosphorus sites is probably due to the long bonds between the capping and the apical palladium atoms, and the angular relationships of the intervening bonds.

Crystallographic Characterisation of $[Pd_{10}(\mu\text{-}CO)_8(\mu_3\text{-}CO)_4(PEt_3)_6]$

Crystals of $[Pd_{10}(\mu\text{-}CO_8(\mu_3\text{-}CO)_4(PEt_3)_6]$ were grown as deep red parallelipipeds, by layer diffusion of diethyl ether into a dichloromethane solution of the compound at room temperature. A crystal of approximate dimensions 0.3 × 0.35 × 0.5 mm was mounted in a glass Lindemann tube and transferred to the goniometer head of an Enraf-Nonius CAD4 diffractometer. Details of the data collection and refinement are summarised in Table II. 11093 reflections were collected in three shells by $w/2\theta$ scans (scan width = $1.00 + 0.35 \tan\theta$) using graphite monochromated Mo Kα radiation, of which 9 956 were considered unique ($R_{\text{merg}} = 0.059$) and 4 609 were considered observed ($I > 3\sigma I$). These were corrected for Lorentz and polarisation effects. No empirical absorption correction was applied. Systematic absences unambiguously determined the space group as $P2_1/n$ (number 14).

Direct methods (SHELXS-86) revealed the ten-palladium metal core of the molecule as the crystallographically independent unit and thus the full molecule occupied one asymmetric unit. The remaining non-hydrogen atoms were located by successive difference Fourier electron density syntheses. The hydrogen atoms were fixed in geometrically idealised positions. The palladium and phosphorus atoms were assigned anisotropic thermal displacement parameters, as were the carbons and oxygens of the CO groups. All other non-hydrogen atoms were given isotropic thermal displacement parameters, and these were allowed to vary independently. The hydrogen atoms were given isotropic thermal parameters according to the atom to which they were attached, but these were not refined. The electron density some distance from the metal core was not well defined, and in order to ensure that the phosphine groups were chemically sensible, their bond lengths and angles were restrained. The P-C bond lengths in the groups were all restrained to 1.87 Å, with a standard deviation of 0.05 Å, and the C-C bond lengths to 1.54 Å, again with a standard deviation of 0.05 Å. All of the bond angles were restrained with a standard deviation of 1°, the Pd-P-C angle to 113°, the P-C-C angle to 110° and C-P-C angle to 105°. An absorption correction using DIFABS was applied to the final model (min/max correction = 0.67/1.48).

Tables III and IV list the important bond lengths and angles for the compound and Table V lists the atomic coordinates. The full molecular structure and labelling scheme is shown in Figure 3, with the hydrogens removed for clarity. A list of the thermal displacement parameters has been deposited with the Editor.

The metal core of the cluster is shown in Figure 2. It is based on a Pd_6 octahedron, with two opposite faces on the upper side capped by single Pd atoms, and two opposite faces on the underside also capped in this way, so that the four bridging atoms are arranged tetrahedrally around the central octahedron.

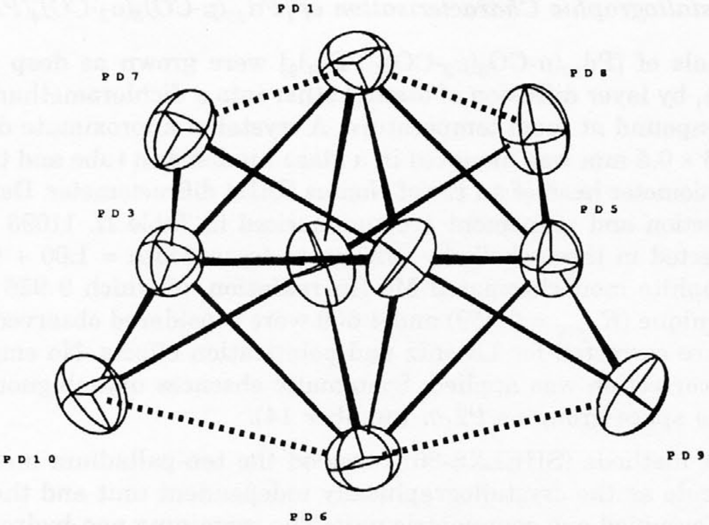

Figure 2. The metal core in $[Pd_{10}(\mu\text{-}CO)_8(\mu_3\text{-}CO)_4(PEt_3)_6]$.

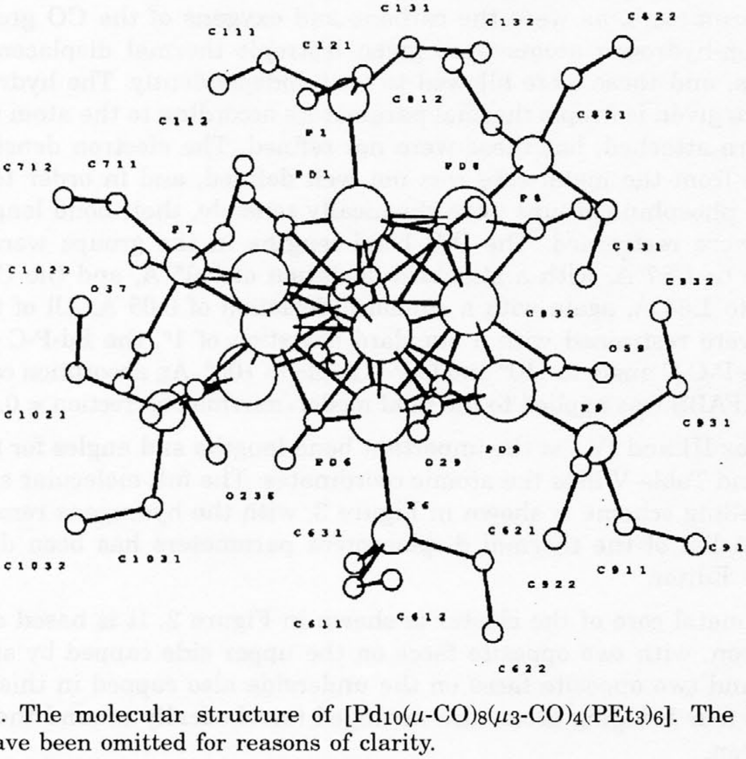

Figure 3. The molecular structure of $[Pd_{10}(\mu\text{-}CO)_8(\mu_3\text{-}CO)_4(PEt_3)_6]$. The hydrogen atoms have been omitted for reasons of clarity.

TABLE III

Bond lengths in [$Pd_{10}(\mu\text{-}CO)_8(\mu_3\text{-}CO)_4(PEt_3)_6$]

Bonds	Length/Å	Bonds	Length/Å
Pd(1)–Pd(2)	2.837(2)	Pd(5)–Pd(9)	2.726(2)
Pd(1)–Pd(3)	2.820(2)	Pd(5)–C(58)	2.13(2)
Pd(1)–Pd(4)	2.842(3)	Pd(5)–C(59)	2.11(2)
Pd(1)–Pd(5)	2.820(2)	Pd(5)–C(125)	2.29(2)
Pd(1)–Pd(8)	3.374(3)	Pd(5)–C(456)	2.41(3)
Pd(1)–P(1)	2.320(8)	Pd(6)–Pd(9)	3.367(3)
Pd(1)–C(125)	2.07(2)	Pd(6)–P(6)	2.333(8)
Pd(1)–C(134)	2.08(2)	Pd(6)–C(236)	2.02(3)
Pd(2)–Pd(3)	2.867(2)	Pd(6)–C(456)	2.07(2)
Pd(2)–Pd(5)	2.831(2)	Pd(7)–P(7)	2.314(6)
Pd(2)–Pd(6)	2.829(2)	Pd(7)–C(27)	2.00(2)
Pd(2)–Pd(7)	2.732(2)	Pd(7)–C(37)	2.06(3)
Pd(2)–Pd(9)	2.732(2)	Pd(8)–P(8)	2.315(7)
Pd(2)–C(27)	2.15(2)	Pd(8)–C(48)	2.02(2)
Pd(2)–C(29)	2.18(3)	Pd(8)–C(58)	1.99(2)
Pd(2)–C(125)	2.31(3)	Pd(9)–P(9)	2.321(7)
Pd(2)–C(236)	2.35(2)	Pd(9)–C(29)	2.04(3)
Pd(3)–Pd(4)	2.835(2)	Pd(9)–C(59)	2.02(2)
Pd(3)–Pd(6)	2.823(2)	Pd(10)–P(10)	2.302(7)
Pd(3)–Pd(7)	2.723(2)	Pd(10)–C(310)	1.97(2)
Pd(3)–Pd(10)	2.727(2)	Pd(10)–C(410)	2.01(2)
Pd(3)–C(37)	2.14(2)	P(1)–C(111)	1.82(3)
Pd(3)–C(134)	2.34(2)	P(1)–C(121)	1.80(3)
Pd(3)–C(236)	2.31(2)	P(1)–C(131)	1.87(4)
Pd(3)–C(310)	2.16(2)	P(6)–C(611)	1.88(3)
Pd(4)–Pd(5)	2.850(2)	P(6)–C(621)	1.90(3)
Pd(4)–Pd(6)	2.823(2)	P(6)–C(631)	1.84(4)
Pd(4)–Pd(8)	2.727(2)	P(7)–C(711)	1.85(2)
Pd(4)–Pd(10)	2.729(2)	P(7)–C(721)	1.87(3)
Pd(4)–C(48)	2.12(2)	P(7)–C(731)	1.87(3)
Pd(4)–C(134)	2.27(2)	P(8)–C(811)	1.86(2)
Pd(4)–C(410)	2.12(2)	P(8)–C(821)	1.90(3)
Pd(4)–C(456)	2.34(3)	P(8)–C(831)	1.89(3)
Pd(5)–Pd(6)	2.847(2)	P(9)–C(911)	1.90(3)
Pd(5)–Pd(8)	2.720(2)	P(9)–C(921)	1.73(3)
P(9)–C(931)	1.97(3)	C(121)–C(122)	1.49(4)
P(10)–C(1011)	1.80(3)	C(131)–C(132)	1.56(4)
P(10)–C(1021)	1.92(3)	C(611)–C(612)	1.53(4)
P(10)–C(1031)	1.89(3)	C(621)–C(622)	1.55(4)
O(27)–C(27)	1.14(2)	C(631)–C(631)	1.51(4)
O(29)–C(29)	1.11(3)	C(711)–C(712)	1.61(3)
O(37)–C(37)	1.12(3)	C(721)–C(722)	1.42(3)
O(48)–C(48)	1.13(3)	C(731)–C(732)	1.46(3)
O(58)–C(58)	1.13(2)	C(811)–C(812)	1.47(3)
O(59)–C(59)	1.13(2)	C(821)–C(822)	1.54(3)
O(125)–C(125)	1.15(2)	C(831)–C(832)	1.42(4)
O(134)–C(134)	1.11(2)	C(911)–C(912)	1.53(4)
O(236)–C(236)	1.16(2)	C(921)–C(922)	1.52(4)
O(310)–C(310)	1.16(3)	C(931)–C(932)	1.53(4)
O(410)–C(410)	1.10(2)	C(1011)–C(1012)	1.52(4)
O(456)–C(456)	1.11(2)	C(1021)–C(1022)	1.53(4)
C(111)–C(112)	1.46(3)	C(1031)–C(1032)	1.61(4)

TABLE IV

Important bond angles in $[Pd_{10}(\mu\text{-}CO)_8(\mu_3\text{-}CO)_4(PEt_3)_6]$

Bonds	Angle/°	Bonds	Angle/°
Pd(3)–Pd(1)–Pd(2)	60.89(6)	Pd(7)–Pd(2)–Pd(3)	58.15(6)
Pd(4)–Pd(1)–Pd(2)	90.46(6)	Pd(9)–Pd(2)–Pd(5)	58.66(6)
Pd(4)–Pd(1)–Pd(3)	60.09(6)	Pd(9)–Pd(2)–Pd(6)	74.50(7)
Pd(5)–Pd(1)–Pd(2)	60.05(6)	Pd(2)–Pd(3)–Pd(1)	59.86(6)
Pd(5)–Pd(1)–Pd(3)	90.82(6)	Pd(4)–Pd(3)–Pd(1)	60.34(6)
Pd(5)–Pd(1)–Pd(4)	60.45(6)	Pd(4)–Pd(3)–Pd(2)	90.01(6)
P(1)–Pd(1)–Pd(2)	133.8(3)	Pd(6)–Pd(3)–Pd(1)	89.72(6)
P(1)–Pd(1)–Pd(3)	134.8(3)	Pd(6)–Pd(3)–Pd(2)	59.64(6)
P(1)–Pd(1)–Pd(4)	135.7(3)	Pd(6)–Pd(3)–Pd(4)	59.86(6)
P(1)–Pd(1)–Pd(5)	134.3(3)	Pd(7)–Pd(3)–Pd(1)	75.91(7)
Pd(3)–Pd(2)–Pd(1)	59.25(6)	Pd(7)–Pd(3)–Pd(2)	58.45(6)
Pd(5)–Pd(2)–Pd(1)	59.68(6)	Pd(10)–Pd(3)–Pd(4)	58.73(6)
Pd(5)–Pd(2)–Pd(3)	89.66(6)	Pd(10)–Pd(3)–Pd(6)	76.04(7)
Pd(6)–Pd(2)–Pd(1)	89.24(7)	Pd(3)–Pd(4)–Pd(1)	59.57(6)
Pd(6)–Pd(2)–Pd(3)	59.41(6)	Pd(5)–Pd(4)–Pd(1)	59.40(6)
Pd(6)–Pd(2)–Pd(5)	60.39(6)	Pd(5)–Pd(4)–Pd(3)	89.90(6)
Pd(7)–Pd(2)–Pd(1)	75.48(7)	Pd(6)–Pd(4)–Pd(1)	89.27(7)
Pd(6)–Pd(4)–Pd(3)	59.85(6)	Pd(4)–Pd(10)–Pd(3)	62.61(6)
Pd(6)–Pd(4)–Pd(5)	60.23(6)	P(10)–Pd(10)–Pd(3)	144.7(3)
Pd(8)–Pd(4)–Pd(1)	74.56(7)	P(10)–Pd(10)–Pd(4)	147.4(3)
Pd(8)–Pd(4)–Pd(5)	58.32(6)	C(111)–P(1)–Pd(1)	114.5(7)
Pd(10)–Pd(4)–Pd(3)	58.66(6)	C(121)–P(1)–Pd(1)	114.0(8)
Pd(10)–Pd(4)–Pd(6)	76.00(7)	C(121)–P(1)–C(111)	105.1(9)
Pd(2)–Pd(5)–Pd(1)	60.28(6)	C(131)–P(1)–Pd(1)	112.9(8)
Pd(4)–Pd(5)–Pd(1)	60.15(6)	C(131)–P(1)–C(111)	104.5(8)
Pd(4)–Pd(5)–Pd(2)	90.42(6)	C(131)–P(1)–C(121)	104.8(9)
Pd(6)–Pd(5)–Pd(1)	89.23(6)	C(611)–P(6)–Pd(6)	113.9(8)
Pd(6)–Pd(5)–Pd(2)	59.78(6)	C(621)–P(6)–Pd(6)	112.7(8)
Pd(6)–Pd(5)–Pd(4)	59.41(6)	C(621)–P(6)–C(611)	105.4(8)
Pd(8)–Pd(5)–Pd(1)	75.03(7)	C(631)–P(6)–Pd(6)	113.4(8)
Pd(8)–Pd(5)–Pd(4)	58.57(6)	C(631)–P(6)–C(611)	104.4(8)
Pd(9)–Pd(5)–Pd(2)	58.85(5)	C(631)–P(6)–C(621)	106.2(9)
Pd(9)–Pd(5)–Pd(6)	74.30(7)	C(711)–P(7)–Pd(7)	113.9(6)
Pd(3)–Pd(6)–Pd(2)	60.95(6)	C(721)–P(7)–Pd(7)	115.0(7)
Pd(4)–Pd(6)–Pd(2)	91.02(6)	C(721)–P(7)–C(711)	106.3(8)
Pd(4)–Pd(6)–Pd(3)	60.28(6)	C(731)–P(7)–Pd(7)	112.3(7)
Pd(5)–Pd(6)–Pd(2)	59.83(6)	C(731)–P(7)–C(711)	105.2(8)
Pd(5)–Pd(6)–Pd(3)	90.22(6)	C(731)–P(7)–C(721)	103.2(8)
Pd(5)–Pd(6)–Pd(4)	60.36(6)	C(811)–P(8)–Pd(8)	115.4(7)
Pd(9)–Pd(6)–Pd(2)	51.43(5)	C(821)–P(8)–Pd(8)	113.9(7)
Pd(9)–Pd(6)–Pd(5)	51.22(5)	C(821)–P(8)–C(811)	105.4(8)
P(6)–Pd(6)–Pd(2)	133.5(3)	C(831)–P(8)–Pd(8)	111.9(7)
P(6)–Pd(6)–Pd(3)	135.9(3)	C(831)–P(8)–C(811)	104.5(8)
P(6)–Pd(6)–Pd(4)	135.8(3)	C(831)–P(8)–C(821)	104.8(8)
P(6)–Pd(6)–Pd(5)	133.8(3)	C(911)–P(9)–Pd(9)	113.1(7)
Pd(3)–Pd(7)–Pd(2)	63.40(6)	C(921)–P(9)–Pd(9)	114.2(8)
P(7)–Pd(7)–Pd(2)	146.4(2)	C(921)–P(9)–C(911)	105.4(8)
P(7)–Pd(7)–Pd(3)	143.7(2)	C(931)–P(9)–Pd(9)	114.0(7)
Pd(5)–Pd(8)–Pd(4)	63.11(6)	C(931)–P(9)–C(911)	103.8(8)
P(8)–Pd(8)–Pd(4)	147.9(2)	C(931)–P(9)–C(921)	105.4(8)
P(8)–Pd(8)–Pd(5)	143.2(2)	C(1011)–P(10)–Pd(10)	115.2(8)
Pd(5)–Pd(9)–Pd(2)	62.49(6)	C(1021)–Pd(10)–Pd(10)	114.1(7)

TABLE IV

(continued)

Bonds	Angle/°	Bonds	Angle/°
P(9)–Pd(9)–Pd(2)	150.1(2)	C(1021)–Pd(10)–C(1011)	105.2(8)
P(9)–Pd(9)–Pd(5)	143.8(3)	C(1031)–P(10)–Pd(10)	112.5(8)
C(1031)–P(10)–C(1011)	104.5(8)	Pd(6)–C(236)–Pd(3)	81.0(8)
C(1031)–P(10)–C(1021)	104.3(8)	O(236)–C(236)–Pd(2)	127.1(21)
Pd(7)–C(27)–Pd(2)	82.3(8)	O(236)–C(236)–Pd3)	126.8(19)
O(27)–C(27)–Pd(2)	130.9(17)	O(236)–C(236)–Pd(6)	142.3(23)
O(27)–C(27)–Pd(7)	146.0(19)	Pd(10)–C(310)–Pd(3)	82.3(9)
Pd(9)–C(29)–Pd(2)	80.7(12)	O(310)–C(310)–Pd(3)	128.2(17)
O(29)–C(29)–Pd(2)	132.4(22)	O(310)–C(310)–Pd10)	149.5(19)
O(29)–C(29)–Pd(9)	146.8(22)	Pd(10)–C(410)–Pd(4)	82.8(8)
Pd(7)–C(37)–Pd(3)	80.8(9)	O(410)–C(410)–Pd(4)	133.5(21)
O(37)–C(37)–Pd(3)	133.9(20)	O(410)–C(410)–Pd(10)	143.5(23)
O(37)–C(37)–Pd(7)	144.8(20)	Pd(5)–C(456)–Pd(4)	73.9(8)
Pd(8)–C(48)–Pd(4)	82.6(9)	Pd(6)–C(456)–Pd(4)	79.4(8)
O(48)–C(48)–Pd(4)	134.0(19)	Pd(6)–C(456)–Pd(5)	78.6(8)
O(48)–C(48)–Pd(8)	143.4(21)	O(456)–C(456)–Pd(4)	127.0(22)
Pd(8)–C(58)–Pd(5)	82.5(8)	O(456)–C(456)–Pd(5)	125.3(19)
O(58)–C(58)–Pd(5)	130.1(16)	O(456)–C(456)–Pd(6)	146.1(26)
O(58)–C(58)–Pd(8)	147.0(19)	C(112)–C(111)–P(1)	109.9(9)
Pd(9)–C(59)–Pd(5)	82.6(8)	C(122)–C(121)–P(1)	110.5(10)
O(59)–C(59)–Pd(5)	132.4(17)	C(132)–C(131)–P(1)	110.3(10)
O(59)–C(59)–Pd(9)	145.1(19)	C(612)–C(611)–P(6)	110.3(10)
Pd(2)–C(125)–Pd(1)	80.4(8)	C(622)–C(621)–P(6)	110.5(9)
Pd(5)–C(125)–Pd(1)	80.3(7)	C(632)–C(631)–P(6)	109.9(10)
Pd(5)–C(125)–Pd(2)	75.8(8)	C(712)–C(711)–P(7)	111.1(9)
O(125)–C(125)–Pd(1)	142.0(20)	C(722)–C(721)–P(7)	110.6(9)
O(125)–C(125)–Pd(2)	125.6(17)	C(732)–C(731)–P(7)	110.7(9)
O(125)–C(125)–Pd(5)	129.1(19)	C(812)–C(811)–P(8)	110.0(9)
Pd(3)–C(134)–Pd(1)	79.1(8)	C(822)–C(821)–P(8)	110.2(9)
Pd(4)–C(134)–Pd(1)	81.5(8)	C(832)–C(831)–P(8)	110.2(10)
Pd(4)–C(134)–Pd(3)	76.0(7)	C(912)–C(911)–P(9)	110.3(9)
O(134)–C(134)–Pd(1)	138.2(21)	C(922)–C(921)–P(9)	109.2(9)
O(134)–C(134)–Pd(3)	127.9(19)	C(932)–C(931)–P(9)	111.4(10)
O(134)–C(134)–Pd(4)	131.2(21)	C(1012)–C(1011)–P(10)	109.0(9)
Pd(3)–C(236)–Pd(2)	75.9(7)	C(1022)–C(1021)–P(10)	111.2(9)
Pd(6)–C(236)–Pd(2)	80.2(8)	C(1032)–C(1031)–P(10)	109.3(10)

The four capping palladiums are each bonded to a terminal phosphine ligand, as are that two palladium atoms which form the apices of the octahedron. Four CO ligands bridge μ_3 fashion across the four uncapped octahedral faces, and the other eight CO's bridge the bonds between the central unit and the capping palladium atoms.

The metal-metal bond lengths in the compound vary over a wide range, from essentially non-bonding at 3.374(3) Å to fairly short, at 2.720(2) Å. Both these extremes are found in the bonds from the capping palladium atoms to the central octahedron, dramatically illustrating the extent of the

TABLE V

Atomic coordinates for [$Pd_{10}(\mu\text{-}CO)_8(\mu_3\text{-}CO)_4(PEt_3)_6$]

Atom	*x*/*a*	*y*/*b*	*z*/*c*	Atom	*x*/*a*	*y*/*b*	*z*/*c*
Pd(1)	0.2640(1)	0.79736(7)	0.52865(8)	C(134)	0.347(2)	0.783(1)	0.611(1)
Pd(2)	0.2895(1)	0.71408(8)	0.43835(7)	C(236)	0.390(2)	0.640(1)	0.481(1)
Pd(3)	0.4102(1)	0.71338(8)	0.55127(7)	C(310)	0.515(1)	0.659(1)	0.604(1)
Pd(4)	0.2447(1)	0.70753(8)	0.61348(7)	C(410)	0.284(2)	0.653(1)	0.689(1)
Pd(5)	0.1248(1)	0.70997(8)	0.50117(7)	C(456)	0.153(2)	0.630(1)	0.570(1)
Pd(6)	0.2724(1)	0.62512(7)	0.52365(8)	C(111)	0.357(2)	0.931(1)	0.579(1)
Pd(7)	0.4600(1)	0.77301(8)	0.45427(8)	C(112)	0.447(3)	0.926(2)	0.553(2)
Pd(8)	0.0719(1)	0.76372(9)	0.60066(8)	C(121)	0.264(2)	0.931(1)	0.457(2)
Pd(9)	0.1294(1)	0.65255(8)	0.39481(7)	C(122)	0.362(4)	0.924(3)	0.438(2)
Pd(10)	0.4121(1)	0.65319(8)	0.65652(7)	C(131)	0.147(3)	0.927(1)	0.557(1)
P(1)	0.2595(8)	0.8978(3)	0.5300(5)	C(132)	0.060(3)	0.921(3)	0.506(2)
P(6)	0.2748(7)	0.5242(3)	0.5183(6)	C(611)	0.364(2)	0.495(1)	0.469(2)
P(7)	0.5894(5)	0.8083(3)	0.4094(3)	C(612)	0.332(3)	0.509(2)	0.403(2)
P(8)	−0.0601(5)	0.7956(4)	0.6451(3)	C(621)	0.154(2)	0.493(1)	0.487(2)
P(9)	0.0339(7)	0.6105(4)	0.3145(4)	C(622)	0.168(3)	0.439(2)	0.447(2)
P(10)	0.5085(6)	0.6180(5)	0.7391(4)	C(631)	0.307(2)	0.489(1)	0.592(2)
O(27)	0.341(1)	0.785(1)	0.3330(7)	C(632)	0.226(4)	0.496(3)	0.630(2)
O(29)	0.299(2)	0.647(1)	0.322(1)	C(711)	0.663(2)	0.862(1)	0.4561(9)
O(37)	0.590(2)	0.787(1)	0.5726(9)	C(712)	0.756(2)	0.881(1)	0.424(1)
O(48)	0.184(1)	0.766(1)	0.7238(8)	C(721)	0.557(2)	0.843(1)	0.334(1)
O(58)	−0.059(1)	0.777(1)	0.4851(8)	C(722)	0.512(3)	0.898(2)	0.341(1)
O(59)	−0.050(1)	0.639(1)	0.4573(9)	C(731)	0.675(2)	0.750(1)	0.393(1)
O(125)	0.137(1)	0.8117(8)	0.4086(7)	C(732)	0.691(3)	0.709(2)	0.444(2)
O(134)	0.386(1)	0.8097(9)	0.6480(8)	C(811)	−0.037(2)	0.812(1)	0.727(1)
O(236)	0.451(1)	0.6160(9)	0.4590(9)	C(812)	0.008(3)	0.869(2)	0.736(1)
O(310)	0.592(1)	0.6471(9)	0.5932(9)	C(821)	−0.118(2)	0.863(1)	0.609(1)
O(410)	0.244(2)	0.634(1)	0.723(1)	C(822)	−0.212(3)	0.877(2)	0.637(2)
O(456)	0.096(1)	0.6058(9)	0.5909(9)	C(831)	−0.160(2)	0.740(1)	0.639(1)
C(27)	0.365(2)	0.767(1)	0.3804(9)	C(832)	−0.121(2)	0.683(2)	0.650(2)
C(29)	0.257(2)	0.659(1)	0.360(1)	C(911)	−0.002(2)	0.533(1)	0.330(1)
C(37)	0.530(2)	0.769(1)	0.541(1)	C(921)	0.088(2)	0.607(1)	0.248(1)
C(48)	0.168(2)	0.754(1)	0.675(1)	C(931)	−0.090(2)	0.650(1)	0.292(1)
C(58)	0.003(2)	0.761(1)	0.5176(8)	C(1011)	0.454(2)	0.616(1)	0.808(1)
C(59)	0.025(1)	0.655(1)	0.4500(8)	C(1021)	0.627(2)	0.660(1)	0.758(1)
C(125)	0.177(2)	0.786(1)	0.4476(9)	C(1031)	0.548(2)	0.541(1)	0.728(1)

asymmetry involved. The weakest interactions are those involving the capping atoms and the apical palladiums and the strongest are with the central atoms of the octahedral unit. The bonds within the octahedron are much more regular in length, with an average of 2.84 Å, are typical for palladium clusters. The structure is very similar to that of the related compound [$Pd_{10}(\mu\text{-}CO)_8(\mu_3\text{-}CO)_4(PBu_3)_6$][5] and the capping groups in particular display a similar asymmetry. The longest bond is 3.421 Å, again to an apical palladium atom, and the shortest is also to a central atom, at 2.694 Å. The average bond length within the octahedral unit is almost identical to [$Pd_{10}(\mu\text{-}CO)_8(\mu_3\text{-}CO)_4((PBu_3)_6$], at 2.83 Å, but the spread of the lengths is much greater. The metal core of the compound [$Pd_8(\mu\text{-}CO)_6(\mu_3\text{-}CO)_2(PMe_3)_7$],[2] is also based on a capped octahedron and this too displays considerable asymmetry in the bonding between the bridging Pd atoms and the octahedral unit. The long and short bonds in this case are 3.318(5) Å and 2.703(5) Å respectively. To further illustrate the effect, the seven atom cluster, $[Pd_7(\mu\text{-}CO)_3(\mu_3\text{-}CO)_4(PMe_3)_7]$,[14] which contains a singly capped octahedral metal core shows slightly less asymmetry, but still displays one long and two short bonds of 3.180(5) Å and 2.729(5) Å associated with the capping atom.

Mednikov and co-workers have previously reported the synthesis of $[Pd_{10}(\mu\text{-}CO)_8(\mu_3\text{-}CO)_4(PEt_3)_6]$,[5] however their characterisation was based only upon IR and chemical analyses data. The compound was synthesised, along with several other clusters, by the reduction of palladium acetate with phosphine ligands, the activity of which was moderated by the presence of acid. The existence and structure of this compound has now been confirmed, and the synthesis reported in this paper represents a new, more viable route into the compound, which can be applied on a much larger scale, to give higher yields of pure product.

The CVE count for the cluster is 136, and the calculated electron count is dependent on the electron contribution associated with the capping atoms. If they are considered to possess three bonds to the central unit, the calculated CVE count is 134, but for only two bonds the count is 142. The first treatment is probably a better representation of the bonding within the cluster, and agrees more closely with the observed count, although as for many palladium clusters, it has proved difficult to predict the exact closed shell requirements of the cluster.[1,15]

Synthesis and Characterisation of $[Pd_{10}(CO)_8(CNXyl)_2(PEt_3)_6]$

Although we have previously studied in some detail the reactions of low nuclearity palladium clusters with isocyanide ligands the corresponding reactions of high nuclearity cluster compounds have been neglected. The palladium cluster described above is effectively sterically saturated and it was of interest to establish the effect of co-ordinating the more sterically demanding isocyanide ligand. When a CH_2Cl_2 solution of 2,6-xylyl isocyanide was added with stirring to a solution of $[Pd_{10}(\mu\text{-}CO)_8(\mu_3\text{-}CO)_4(PEt_3)_6]$, the solution changed in colour immediately from a deep red/purple to dark red, and this was accompanied by some effervescence which lasted for only a few seconds. The solution was allowed to continue stirring for five minutes and the solvent was removed under reduced pressure. The crude product was soluble in all commonly available laboratory solvents, but recrystallisation was effected from a highly concentrated hexane solution, with cooling, giving red single crystals. Indeed the relatively low yield of the product is a reflection of the compounds great solubility even in non-polar solvents.

The compound was very air sensitive and accurate chemical analyses proved impossible to obtain. However, $^{31}P\{^1H\}$-NMR and IR spectra were obtained. The IR spectrum revealed three different ν(C-O) stretching frequencies at 1951(m), 1845(m) and 1723(m) cm^{-1}, consistent with the presence of both μ_2- and μ_3-bridging CO ligands. The presence of briding isocyanide we also indicated by a band at 2086(m) cm^{-1}. This frequency suggests the presence of a bridging isocyanide ligand with a linear geometry.[4] This has subsequently been confirmed by the single crystal analysis described below. Additional bands in the IR indicated the presence of the PEt_3 ligand.

The quantity of crystalline product obtained from the reaction precluded an NMR study of the pure material, however, the solution $^{31}P\{^1H\}$-NMR spectrum of the crude product revealed a singlet at –14.6 ppm. This did not broaden or collapse at low temperature suggesting the cluster is fluxional, reorganising *via* a low energy process. Thus no structural conclusions could be drawn from the analysis of the spectral data.

Crystallographic Characterisation of $[Pd_{10}(\mu\text{-}CO)_6(\mu_3\text{-}CO)_2(\mu\text{-}CNXyl)_2(PEt_3)_6]$

Crystals of $[Pd_{10}(\mu\text{-}CO)_6(\mu_3\text{-}CO)_2(\mu\text{-}CNXyl)_2(PEt_3)_6]$ were grown as deep red parallelipipeds, by precipitation from a hexane solution of the compound, at a temperature of –10 °C. A crystal of approximate dimensions 0.3 × 0.3 × 0.5 mm was mounted in a glass Lindemann tube, with a small quantity of hexane solvent, and transferred to the goniometer head of an Enraf-Nonius CAD4 diffractometer. Details of the data collection and refinement are summarised in Table VI. 3443 reflections were collected in two shells by ω scans (scan width = 1.00 + 0.35 tan θ) using graphite monochromated Mo Kα radiation, of which 2 831 were considered unique ($R_{\text{merg}} = 0.139$) and 1 515 were considered observed ($I > 3\sigma I$). These were corrected for Lorentz and polarisation effects. No empirical absorption correction was applied. Systematic absences unambiguously determined the space group as *C*2/*c* (number 15).

Direct methods (SHELXS-86) revealed half the metal core of the molecule as the crystallographically independent unit and thus the full molecule occupied two asymmetric units. The remaining non-hydrogen atoms were located by successive difference Fourier electron density syntheses. The hydrogen atoms were fixed in geometrically idealised positions. The palladium and phosphorus atoms were assigned anisotropic displacement parameters, whilst all other non-hydrogen atoms were given isotropic displacement parameters, and these were allowed to vary independently. The hydrogen atoms were given isotropic thermal parameters according to the atom to which they were attached, but these were not refined.

During the second shell of the data collection, the crystal quality became so poor that further data collection was impossible, due to loss of solvent from the crystal over a period of days. The data set was thus not as good

TABLE VI

Crystallographic data for the compound $[Pd_{10}(\mu\text{-}CO)_6(\mu_3\text{-}CO)_2(\mu\text{-}CNXyl)_2(PEt_3)_6]$

General details	
Formula	$C_{62}H_{108}N_2O_8P_6Pd_{10}$
Molecular weight	2259.4
D_c/g cm^{-3}	1.76
$F(000)$	4432
Linear abs. coefficient/cm^{-1}	21.9
Crystal colour	Deep red
Cell details	
Crystal system	Monoclinic
Space group	$C2/c$
a/Å	22.59(3)
b/Å	17.81(3)
c/Å	21.34(2)
α/°	90
β/°	94.46(9)
g/°	90
V/Å^3	8551.6
Z	4
Data collection	
X-radiation	Mo Kα, λ= 0.71069 Å
$\theta_{\min}$, $\theta_{\max}$/°	0, 21
Min., max. h,k,l	1, 22; –1, 17; –21, 21
ω-scan width/°	1.00 + 0.35 tanθ
Horizontal aperture/mm	3.5
Total data collected	3443
Total unique data	2831
Total observed data	1515
Merging R factor	0.14
Refinement	
Absorption correction	DIFABS (min/max = 0.77/1.26)
Number of parameters	213
Ratio data: parameters	7.62
Weighting scheme	Tukey and Prince (3, 4, -0.1., 3.2)
Final R factor	0.14
Final R_w	0.16

as might have been hoped and as a result, the electron density some distance from the metal core was not well defined. In order to ensure that the phosphine groups were chemically sensible, their bond lengths and angles were restrained, as for $[Pd_{10}(\mu\text{-}CO)_8(\mu_3\text{-}CO)_4(PEt_3)_6]$. The P-C bond lengths in the phosphine groups were all restrained to 1.87 Å, with a standard de-

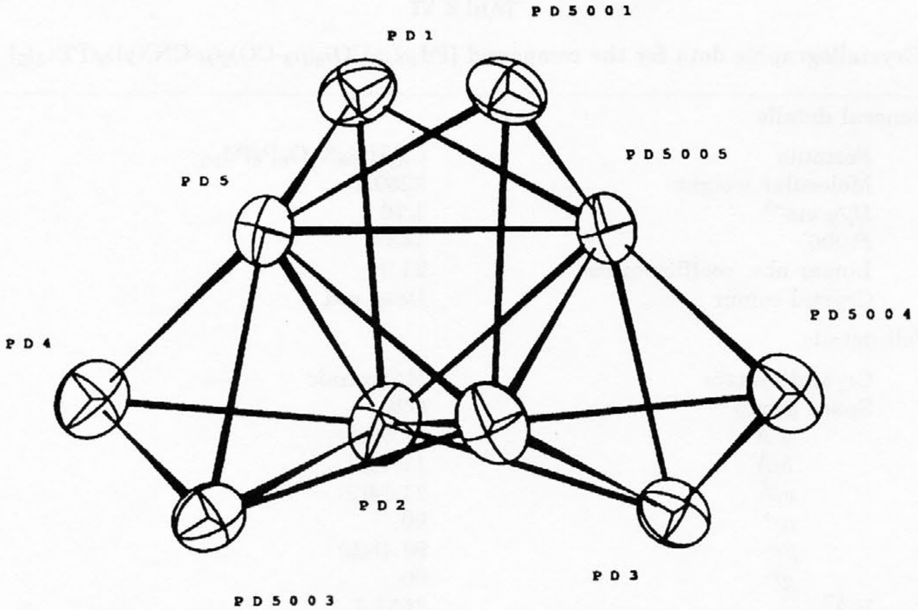

Figure 4. The metal core in $[Pd_{10}(\mu\text{-}CO)_6(\mu_3\text{-}CO)_2(\mu\text{-}CNXyl)_2(PEt_3)_6]$.

viation of 0.05 Å, and the C-C bond lengths to 1.54 Å, again with a standard deviation of 0.05 Å. All of the bond angles were restrained with a standard deviation of 1°, the Pd-P-C angle to 113°, the P-C-C angle to 110° and the C-P-C angle to 105°. An absorption correction using DIFABS was applied to the final model (min/max correction = 0.77/1.26).

The metal core of the cluster is shown in Figure 4. It is based on a Pd_8 tetracapped tetrahedral unit, which possesses two further capping atoms, that break the tetrahedral symmetry of the core, leaving it with just two-fold axial symmetry. This is crystallographically imposed, because the molecule lies on a C_2 rotation axis.

The full molecular structure and labelling scheme for the cluster are shown in Figure 5, with the hydrogen atoms removed for clarity. Tables VII and VIII list important bond lengths and angles, whilst Table IX lists the atomic coordinates. A list of the thermal displacement parameters has been deposited with the Editor. Each capping palladium (*i.e.*, all atoms except those comprising the central Pd_4 unit) is bonded to a terminal phosphine so that the compound has six phosphine groups, the same number as in the parent cluster, $[Pd_{10}(\mu\text{-}CO)_8(\mu_3\text{-}CO)_4(PEt_3)_6]$.

Two μ_3-bridging CO ligands are coordinated each to one palladium atom in the central tetrahedron and to two of the capping palladiums, and the two xylyl isocyanide groups bridge μ_2- fashion across a central and a capping

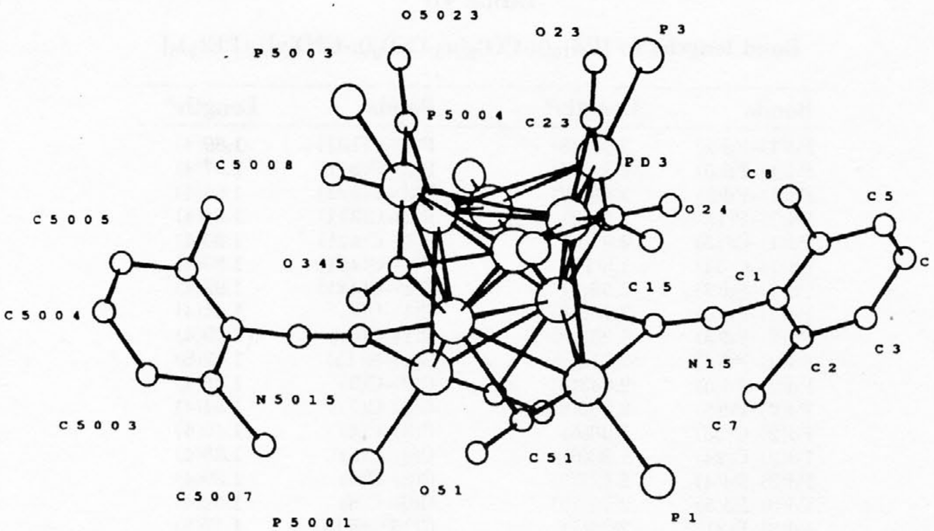

Figure 5. A more complete illustration of the molecular structure of $[Pd_{10}(\mu\text{-}CO)_6(\mu_3\text{-}CO)_2(\mu\text{-}CNXyl)_2(PEt_3)_6]$. The ethyl groups and hydrogen atoms have been omitted for reasons of clarity.

palladium on the under side of the cluster. Six μ_2-CO ligands are situated across the remaining radial Pd-Pd bonds, completing the structure.

Because of the difficulty in collecting a full data set, the quality of the structure was relatively poor, and the quoted bond lengths and angles possess high standard deviations. However, from the data, it was possible to make out all the ligands surrounding the core and thus to complete a full structural characterisation.

The bond lengths, although inaccurately determined, are within the usual limits for Pd-Pd bonds in cluster compounds, ranging from 3.34(1) Å (essentially non-bonding) to 2.707(8) Å. The central tetrahedral unit is very asymmetrical, being open on the underside of the cluster, with one very long bond of 3.34(1) Å. The four capping atoms are also asymmetrically bonded, with (as for many capped palladium clusters) one long bond and two much shorter bonds. The longer bonds range from 3.253(8) to 2.989(8) Å and the shorter range from 2.827(7) to 2.707(8) Å, whilst the bonds forming the tetrahedron lie between these two ranges at an average of 2.84 Å. This is directly comparable with the range of bond lengths found in the compound $[Pd_{10}(\mu\text{-}CO)_8(\mu_3\text{-}CO)_4(PEt_3)_6]$ described above.

This metal core geometry has never previously been reported in palladium cluster chemistry, or indeed for any transition metal and all other known decanuclear palladium compounds have structures based on a cen-

TABLE VII

Bond lengths in $[Pd_{10}(\mu\text{-}CO)_6(\mu_3\text{-}CO)_2(\mu\text{-}CNXyl)_2(PEt_3)_6]$

Bonds	Length/°	Bonds	Length/°
Pd(1)–Pd(2)	2.989(8)	P(1)–C(131)	1.89(4)
Pd(1)–Pd(5)	2.712(7)	P(3)–C(311)	1.87(4)
Pd(1)–Pd(5)	2.804(7)	P(3)–C(321)	1.85(4)
Pd(1)–P(1)	2.25(2)	P(3)–C(331)	1.84(4)
Pd(1)–C(15)	2.07(6)	P(4)–C(411)	1.85(4)
Pd(1)–C(51)	1.6(1)	P(4)–C(421)	1.83(4)
Pd(2)–Pd(2)	2.99(1)	P(4)–C(431)	1.92(4)
Pd(2)–Pd(3)	2.755(8)	C(1)–C(2)	1.41(4)
Pd(2)–Pd(3)	3.253(8)	C(1)–C(6)	1.39(4)
Pd(2)–Pd(4)	2.711(8)	C(1)–N(15)	1.42(6)
Pd(2)–Pd(5)	2.843(8)	C(2)–C(3)	1.38(4)
Pd(2)–Pd(5)	2.830(8)	C(2)–C(7)	1.54(4)
Pd(2)–C(23)	1.96(5)	C(3)–C(4)	1.40(4)
Pd(2)–C(24)	1.86(6)	C(4)–C(5)	1.38(4)
Pd(3)–Pd(4)	2.827(7)	C(5)–C(6)	1.39(4)
Pd(3)–Pd(5)	2.707(8)	C(6)–C(8)	1.52(4)
Pd(3)–P(3)	2.28(2)	C(15)–N(15)	1.17(5)
Pd(3)–C(23)	2.02(5)	C(23)–O(23)	1.23(6)
Pd(3)–C(345)	2.13(7)	C(24)–O(24)	1.20(6)
Pd(4)–Pd(5)	2.771(7)	C(111)–C(112)	1.60(4)
Pd(4)–P(4)	2.35(3)	C(121)–C(122)	1.51(5)
Pd(4)–C(24)	2.09(6)	C(131)–C(132)	1.51(5)
Pd(4)–C(345)	2.17(6)	C(311)–C(312)	1.50(4)
Pd(5)–Pd(5)	3.34(1)	C(321)–C(322)	1.55(4)
Pd(5)–C(15)	2.12(5)	C(331)–C(332)	1.53(4)
Pd(5)–C(51)	2.26(7)	C(345)–O(345)	1.10(6)
Pd(5)–C(345)	2.55(7)	C(411)–C(412)	1.48(4)
P(1)–C(111)	1.82(4)	C(421)–C(422)	1.53(5)
P(1)–C(121)	1.89(4)	C(431)–C(432)	1.54(5)

tral octahedral unit. The CVE count for the compound is 132, and this agrees exactly with the calculated count required for a hexacapped tetrahedron (60 + 6 x 12) although this is likely to be fortuitous in the light of other such calculation on similar palladium clusters.[15]

The synthesis of the compound is based upon an interesting class of ligand substitution reaction, not often seen in palladium cluster chemistry. Each of the two xylyl isocyanide molecules replaces two CO ligands in the reaction, and it is this that leads to a reduction in the CVE count from the starting material to the product, and thus ultimately to a change in the shape of the cluster. The driving force for this double substitution is likely to have a steric origin, since the CO ligand is much smaller than xylyl isocyanide. The reaction reveals a new and subtle possibility for the control of geometry in palladium clusters. By the substitution of one ligand for another of differing size, it may in future be possible to alter the number of ligands surrounding the metal core, and thus indirectly change its shape.

TABLE VIII

Important bond angles in $[Pd_{10}(\mu\text{-}CO)_6(\mu_3\text{-}CO)_2(\mu\text{-}CNXyl)_2(PEt_3)_6]$

Bonds	Angle/°	Bonds	Angle/°
Pd(5)–Pd(1)–Pd(2)	59.6(2)	Pd(5)–Pd(4)–Pd(3)	57.8(2)
Pd(5)–Pd(1)–Pd(2)	58.4(2)	P(4)–Pd(4)–Pd(2)	146.5(6)
Pd(5)–Pd(1)–Pd(5)	74.6(2)	P(4)–Pd(4)–Pd(3)	129.9(7)
P(1)–Pd(1)–Pd(2)	146.6(7)	P(4)–Pd(4)–Pd(5)	147.9(7)
P(1)–Pd(1)–Pd(5)	146.7(6)	Pd(1)–Pd(5)–Pd(1)	82.4(2)
P(1)–Pd(1)–Pd(5)	132.0(7)	Pd(2)–Pd(5)–Pd(1)	65.0(2)
Pd(2)–Pd(2)–Pd(1)	96.2(1)	Pd(2)–Pd(5)–Pd(1)	64.1(2)
Pd(3)–Pd(2)–Pd(1)	110.9(3)	Pd(2)–Pd(5)–Pd(2)	63.5(2)
Pd(3)–Pd(2)–Pd(2)	68.9(2)	Pd(3)–Pd(5)–Pd(1)	135.6(3)
Pd(3)–Pd(2)–Pd(1)	106.9(2)	Pd(3)–Pd(5)–Pd(1)	118.4(2)
Pd(3)–Pd(2)–Pd(2)	52.2(2)	Pd(3)–Pd(5)–Pd(2)	71.7(2)
Pd(3)–Pd(2)–Pd(3)	111.7(2)	Pd(3)–Pd(5)–Pd(2)	59.6(2)
Pd(4)–Pd(2)–Pd(1)	81.8(2)	Pd(4)–Pd(5)–Pd(2)	57.7(2)
Pd(4)–Pd(2)–Pd(2)	103.3(3)	Pd(4)–Pd(5)–Pd(3)	62.1(2)
Pd(4)–Pd(2)–Pd(3)	55.7(2)	Pd(5)–Pd(5)–Pd(1)	54.0(2)
Pd(5)–Pd(2)–Pd(1)	55.4(2)	Pd(5)–Pd(5)–Pd(1)	51.5(2)
Pd(5)–Pd(2)–Pd(2)	58.0(2)	Pd(5)–Pd(5)–Pd(2)	53.7(2)
Pd(5)–Pd(2)–Pd(3)	52.2(2)	Pd(5)–Pd(5)–Pd(2)	54.1(2)
Pd(5)–Pd(2)–Pd(4)	59.8(2)	C(111)–P(1)–Pd(1)	114.4(8)
Pd(5)–Pd(2)–Pd(1)	57.5(2)	C(121)–P(1)–Pd(1)	113.1(9)
Pd(5)–Pd(2)–Pd(2)	58.5(2)	C(121)–P(1)–C(111)	104.3(9)
Pd(5)–Pd(2)–Pd(3)	58.0(2)	C(131)–P(1)–Pd(1)	113.5(8)
Pd(5)–Pd(2)–Pd(5)	72.2(3)	C(131)–P(1)–C(111)	105.3(9)
Pd(2)–Pd(3)–Pd(2)	58.9(2)	C(131)–P(1)–C(121)	105.2(9)
Pd(4)–Pd(3)–Pd(2)	106.4(2)	C(311)–P(3)–Pd(3)	113.9(8)
Pd(4)–Pd(3)–Pd(2)	52.4(2)	C(321)–P(3)–Pd(3)	113.2(8)
Pd(5)–Pd(3)–Pd(2)	62.4(2)	C(321)–P(3)–C(311)	105.5(9)
Pd(5)–Pd(3)–Pd(2)	56.1(2)	C(331)–P(3)–Pd(3)	112.8(8)
Pd(5)–Pd(3)–Pd(4)	60.0(2)	C(331)–P(3)–C(311)	105.0(9)
P(3)–Pd(3)–Pd(2)	143.0(5)	C(331)–P(3)–C(321)	105.6(9)
P(3)–Pd(3)–Pd(2)	135.5(5)	C(411)–P(4)–Pd(4)	113.2(8)
P(3)–Pd(3)–Pd(4)	105.6(5)	C(421)–P(4)–Pd(4)	113.5(8)
P(3)–Pd(3)–Pd(5)	153.4(6)	C(421)–P(4)–C(411)	105.7(9)
Pd(3)–Pd(4)–Pd(2)	71.9(2)	C(431)–P(4)–Pd(4)	113.7(9)
Pd(5)–Pd(4)–Pd(2)	62.5(2)	C(431)–P(4)–C(411)	104.9(9)
C(431)–P(4)–C(421)	105.1(9)	O(24)–C(24)–Pd(2)	141.6(55)
C(6)–C(1)–C(2)	120.0(8)	O(24)–C(24)–Pd(4)	132.0(51)
N(15)–C(1)–C(2)	120.3(30)	Pd(5)–C(51)–Pd(1)	87.2(36)
N(15)–C(1)–C(6)	119.7(30)	O(51)–C(51)–Pd(5)	98.1(53)
C(3)–C(2)–C(1)	119.7(8)	C(112)–C(111)–P(1)	109.5(10)
C(7)–C(2)–C(1)	120.1(8)	C(122)–C(121)–P(1)	110.3(10)
C(7)–C(2)–C(3)	119.9(9)	C(132)–C(131)–P(1)	110.2(10)
C(4)–C(3)–C(2)	119.8(9)	C(312)–C(311)–P(3)	110.2(10)
C(5)–C(4)–C(3)	120.0(9)	C(322)–C(321)–P(3)	110.1(10)
C(6)–C(5)–C(4)	120.0(9)	C(332)–C(331)–P(3)	109.8(10)
C(5)–C(6)–C(1)	119.9(8)	Pd(4)–C(345)–Pd(3)	82.3(26)
C(8)–C(6)–C(1)	119.9(9)	Pd(5)–C(345)–Pd(3)	70.1(20)
C(8)–C(6)–C(5)	119.8(9)	Pd(5)–C(345)–Pd(4)	71.5(20)
Pd(5)–C(15)–Pd(1)	83.9(20)	O(345)–C(345)–Pd(3)	136.6(50)
N(15)–C(15)–Pd(1)	144.6(42)	O(345)–C(345)–Pd(4)	141.0(52)
N(15)–C(15)–Pd(5)	129.0(42)	O(345)–C(345)–Pd(5)	118.0(49)
Pd(3)–C(23)–Pd(2)	87.7(22)	C(412)–C(411)–P(4)	109.9(10)
O(23)–C(23)–Pd(2)	129.9(44)	C(422)–C(421)–P(4)	109.8(10)
O(23)–C(23)–Pd(3)	142.2(44)	C(432)–C(431)–P(4)	110.3(10)
Pd(4)–C(24)–Pd(2)	86.3(22)	C(15)–N(15)–C(1)	166.4(50)

TABLE IX

Atomic coordinates for $[Pd_{10}(\mu\text{-}CO)_6)(\mu_3\text{-}CO)_2(\mu\text{-}CNXyl)_2(PEt_3)_6]$

Atom	x/a	y/b	z/c	Atom	x/a	y/b	z/c
Pd(1)	0.0364(3)	0.2126(3)	0.1768(2)	C(121)	–0.007(3)	0.038(3)	0.118(3)
Pd(2)	0.0270(3)	0.3795(3)	0.1881(2)	C(122)	–0.067(3)	0.068(5)	0.097(7)
Pd(3)	–0.0902(3)	0.4251(3)	0.1747(2)	C(131)	0.049(3)	0.141(3)	0.027(2)
Pd(4)	0.1451(3)	0.3658(3)	0.2211(2)	C(132)	0.086(4)	0.211(5)	0.019(3)
Pd(5)	0.0678(2)	0.2828(3)	0.2879(2)	C(311)	–0.217(2)	0.487(2)	0.086(2)
P(1)	0.051(1)	0.115(1)	0.113(1)	C(312)	–0.199(3)	0.463(5)	0.023(3)
P(3)	–0.1510(9)	0.520(2)	0.1365(9)	C(321)	–0.113(2)	0.588(2)	0.088(2)
P(4)	0.242(1)	0.383(2)	0.191(1)	C(322)	–0.155(3)	0.653(3)	0.068(4)
C(1)	–0.099(2)	0.278(3)	0.020(2)	C(331)	–0.182(2)	0.575(3)	0.199(2)
C(2)	–0.148(2)	0.231(3)	0.006(2)	C(332)	–0.131(3)	0.607(5)	0.244(3)
C(3)	–0.186(3)	0.245(4)	–0.047(3)	C(345)	0.164(3)	0.351(4)	0.322(3)
C(4)	–0.177(3)	0.308(4)	–0.084(3)	C(411)	0.299(2)	0.328(3)	0.239(2)
C(5)	–0.126(3)	0.350(4)	–0.074(3)	C(412)	0.280(3)	0.249(3)	0.243(4)
C(6)	–0.088(2)	0.337(3)	–0.021(2)	C(421)	0.251(2)	0.355(4)	0.109(2)
C(7)	–0.163(3)	0.169(4)	0.053(3)	C(422)	0.296(5)	0.407(5)	0.080(3)
C(8)	–0.039(3)	0.394(4)	–0.002(4)	C(431)	0.270(2)	0.485(3)	0.197(3)
C(15)	–0.034(2)	0.261(3)	0.123(2)	C(432)	0.224(4)	0.538(3)	0.162(6)
C(23)	–0.011(2)	0.477(3)	0.169(2)	O(23)	0.012(2)	0.539(3)	0.162(2)
C(24)	0.091(3)	0.393(3)	0.140(3)	O(24)	0.103(2)	0.406(3)	0.086(3)
C(51)	0.089(4)	0.183(4)	0.227(4)	O(51)	0.135(3)	0.157(4)	0.262(3)
C(111)	0.122(2)	0.066(3)	0.131(2)	O(345)	0.196(2)	0.323(3)	0.356(2)
C(112)	0.120(3)	–0.014(3)	0.097(4)	N(15)	–0.059(2)	0.264(2)	0.073(2)

This represents a much milder and more subtle approach to the problem than the use of redox reagents, which are likely to destroy this type of compound.

Synthesis and Characterisation of $[Pd_5(\mu\text{-}SO_2)_2(\mu_3\text{-}SO_2)_2(PEt_3)_5]$

We have shown previously[16] that $[Pd_8(\mu\text{-}CO)_6(\mu_3\text{-}CO)_2(PMe_3)_7]$ reacts with sulphur dioxide to form pentanuclear palladium complexes, so it was decided to investigate the reaction of $[Pd_{10}(\mu\text{-}CO)_8(\mu_3\text{-}CO)_4(PEt_3)_6]$ with SO_2, to determine whether a similar product would result. In parallel with this investigation, the reaction of $[Pd_2(dba)_3].CHCl_3$ with SO_2 and the phosphine, PEt_3, was also carried out, as this general reaction has been shown to produce the same pentanuclear palladium complexes.[3]

When SO_2 was bubbled through a CH_2Cl_2 solution of $[Pd_{10}(\mu\text{-}CO)_8(\mu_3\text{-}CO)_4(PEt_3)_6]$ the mixture changed colour gradually, from deep red/purple to deep red. After stirring for an hour, the solvent was removed under reduced pressure and the product extracted from the mixture with several portions of Et_2O. The solution was concentrated by removing Et_2O under reduced pressure, yielding deep red microcrystals of the product, $[Pd_5(\mu\text{-}SO_2)_2(\mu_3\text{-}SO_2)_2(PEt_3)_5]$. The same product was obtained by the second reaction. When a THF solution of PEt_3

was added to a CH_2Cl_2 solution of $[Pd_2(dba)_3].CHCl_3$, and SO_2 was bubbled through it, the colour of the solution changed gradually from purple to deep red. The solvent was then removed under reduced pressure and the crude product washed with several portions of hexane to remove the dba. Recrystallisation from a concentrated solution in Et_2O gave a deep red microcrystalline product, which could not be fully separated from a dba impurity, but analysed satisfactorily for $[Pd_5(SO_2)_4(PEt_3)_5]{\cdot}0.61$dba.

The infra-red spectrum of the compound revealed four $\nu(SO_2)$ stretching frequencies, at 1185(m), 1164(m), 1061(s) and 1050(m) cm^{-1}. This is consistent with the presence of bridging SO_2 ligands.

The $^{31}P\{^1H\}$-NMR data for the compound are summarised in Figure 6 together with the proposed structure. These are consistent with other NMR data for related pentapalladium clusters containing alternative phosphine ligands,[1,3] with a distorted trigonal bipyramidal structure. The phosphorus atoms attached to the axial palladium atoms do not couple to the other phosphorus atoms. Coupling is observed only between the two equivalent and one unique equatorial phosphorus atoms, giving rise to the singlet, doublet, triplet structure. The lack of coupling to the phosphines on the axial palladium atoms is probably a combination of the extra length of the Pd_{ax}-Pd_{eq} bonds (3.410(5) Å in $[Pd_5(\mu\text{-}SO_2)_2(\mu_3\text{-}SO_2)_2(PMe_3)_5]$,[16] and the angular relationship of the Pd-P bonds.

The coordination of the four SO_2 ligands in these compounds has previously been shown to be rather unusual, two exhibiting the usual μ_2 bridging mode, as is normal, but two bridging in a μ_3 fashion, through two S-Pd bonds and one O-Pd bond. This renders one of the three equatorial palladium atoms unequal to the other two, leaving the molecule with just a one axis of symmetry, a C_2 rotation axis through the unique Pd atom.

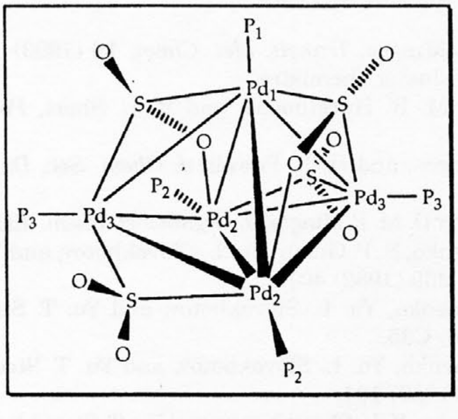

values

$\delta P_1 = 6.1$ ppm (t, 1P)

$\delta P_2 = 13.7$ ppm (d, 2P)

$\delta P_3 = 19.3$ ppm (s, 2P)

Coupling constant

$^3J_{P_1\text{-}P_2} = 29$ Hz

Figure 6. The proposed structure of $[Pd_5(\mu\text{-}SO_2)_2(\mu_3\text{-}SO_2)_2(PEt_3)_5]$ and the assignment of its $^{31}P\{^1H\}$-NMR spectrum.

The compound $[Pd_5(\mu\text{-}SO_2)_2(\mu_3\text{-}SO_2)_2(PEt_3)_5]$ is one of a series of pentapalladium clusters $[Pd_5(\mu\text{-}SO_2)_2(\mu_3\text{-}SO_2)_2(PR_3)_5]$, which have recently been produced. These clusters all possess distorted metal cores, their structures ranging from almost square pyramidal,[16] to approximately trigonal bipyramidal.[3] All are thought to display the unusual μ_3-SO_2 coordination, and the degree of core distortion, away from the expected trigonal bipyramidal, depends on the cone angles and basicities of the phosphine ligands attached. Thus, for phosphines with small cone angles, such as PMe_3, the structure is close to the square based pyramid, but when the much larger triphenylarsine ligand is involved, the structure is almost trigonal bipyramidal.

The compound $[Pd_5(\mu\text{-}SO_2)_2(\mu_3\text{-}SO_2)_2(PEt_3)_5]$ is produced only in low yield from the reaction of $[Pd_{10}(\mu\text{-}CO)_8(\mu_3\text{-}CO)_4(PEt_3)_6]$ with SO_2, and the reaction with $[Pd_2(dba)_3]\cdot CHCl_3$, SO_2 and PEt_3 provides a much more viable route into the cluster, despite the difficulty in removing the dba ligand from the product. The first synthesis however, shows an interesting parallel with a related reaction, between the cluster $[Pd_8(\mu\text{-}CO)(\mu_3\text{-}CO)_2(PMe_3)_7]$ and SO_2 from which a similar product, $[Pd_5(\mu\text{-}SO_2)_2(\mu_3\text{-}SO_2)_2(PMe_3)_5]$ is formed.

Supplementary Materials. – Crystallographic data (excluding structure factors which are available from the authors) for the structures reported in this paper have been deposited with the Cambridge Crystallographic Data Centre as supplementary publication no. CCDC-109/68-745. Copies of the data can be obtained on application to the Director, CCDC, 12 Union Road, Cambridge CB2 1EZ, UK. (Fax: 44 (0) 1223-336033; E-mail: teched@chemcrys.cam.ac.uk).

Acknowledgements. – The SERC is thanked for financial support and British Petroleum plc for endowing DMPM's Chair at Imperial College.

REFERENCES

1. A. D. Burrows and D. M. P. Mingos, *Transit. Met. Chem.* **18** (1993) 129 gives a general review of palladium cluster chemistry.
2. M. Bochmann, I. Hawkins, M. B. Hursthouse, and R. L. Short, *Polyhedron* **6** (1987) 1987.
3. A. D. Burrows, D. M. P. Mingos, and H. R. Powell, *J. Chem. Soc. Dalton Trans.* (1992) 261.
4. A. D. Burrows, H. Fleischer, and D. M. P. Mingos, *J. Organomet. Chem.* **433** (1992) 311.
5. E. G. Mednikov, N. K. Eremenko, S. P. Gubin, Yu. L. Slovokhotov, and Yu. T. Struchkov, *J. Organomet. Chem.* **239** (1982) 401.
6. E. G. Mednikov, N. K. Eremenko, Yu. L. Slovokhotov, and Yu. T. Struchkov, *J. Organomet. Chem.* **301** (1986) C35.
7. E. G. Mednikov, N. K. Eremenko, Yu. L. Slovokhotov, and Yu. T. Struchkov, *Zh. Vsas. Khim. Mendeleeva* **32** (1987) 101.
8. E. G. Mednikov, N. K. Eremenko, Y. L. Slovokhotov, and Yu. T. Struchkov, *J. Chem. Soc. Chem. Commun.* (1987) 218.
9. E. G. Mednikov, Y. L. Slovokhotov, and Yu. T. Struchkov, *Metallorg. Khim.* **4** (1991) 123.

10. E. G. Mednikov, N. K. Eremenko, Yu. L. Slovokhotov, Yu. T. Struchkov, and S. P. Gubin, *J. Organomet. Chem.* **258** (1983) 247.
11. G. M. Sheldrick, SHELX 86 (1986). Program for Crystal Structure Determinations. University of Gottingen.
12. D. J. Watkin, J. R. Carruthers, and R. W. Betteridge, *CRYSTALS, User Manual*, Chemical Crystallography Laboratory, University of Oxford, 1985.
13. International Tables for X-ray Crystallography, Kynoch Press, Birmingham, 1974.
14. R. Goddard, P. W. Jolly, C. Krüger, K.-P. Schick, and G. Wilke, *Organometallics* **1** (1982) 1709.
15. D. M. P. Mingos and D. J. Wales, *Introduction to Cluster Chemistry*, Prentice Hall, New York, 1990.
16. S. G. Bott, O. J. Ezomo, and D. M. P. Mingos, *J. Chem. Soc. Chem. Commun.* (1988) 1048.

SAŽETAK

Sinteza i karakterizacija $[\mathrm{Pd_{10}}(\mu\text{-CO})_8(\mu_3\text{-CO})_4(\mathrm{PEt_3})_6]$ i $[\mathrm{Pd_{10}}(\mu\text{-CO})_6(\mu_3\text{-CO})_2(\mu\text{-CNXylyl})_2(\mathrm{PEt_3})_6]$

D. Michael P. Mingos i Christopher M. Hill

Priređeni su dekanuklearni paladijevi klusteri sastava $[\mathrm{Pd_{10}}(\mu\text{-CO})_8(\mu_3\text{-CO})_4\,(\mathrm{PEt_3})_6]$ i $[\mathrm{Pd_{10}}(\mu\text{-CO})_6(\mu_3\text{-CO})_2(\mu\text{-CNXyl})_2(\mathrm{PEt_3})_6]$ (Xyl = $\mathrm{C_6H_3Me_2}$-2,6). Spojevi su karakterizirani spektroskopskim podacima i rentgenskom strukturnom analizom na monokristalu. Prvi od dva navedena spoja ima deformiranu četveroplošno centriranu oktaedarsku geometriju, a drugi troplošno (tri skupine $\mathrm{Pd_2}$ iznad 3 plohe) centriranu tetraedarsku geometriju. Ovaj posljednji spoj jedinstven je u kemiji klustera: strukturne promjene, izazvane u njemu dodatkom izocijanida, zanimljiv su primjer utjecaja steričkih zahtjeva izocijanidnog liganda koji utječe na ukupan broj elektrona i geometriju klustera. Spoj $[\mathrm{Pd_{10}}(\mu\text{-CO})_8(\mu_3\text{-CO})_4(\mathrm{PEt_3})_6]$ reagira sa $\mathrm{SO_2}$ i daje $[\mathrm{Pd_5}(\mu\text{-SO_2})_2(\mu_3\text{-SO_2})_2(\mathrm{PEt_3})_5]$.